



Brief Communication: Representation of heat conduction into the ice in marine ice shelf melt modeling

Jonathan Wiskandt^{1,2} and Nicolas C. Jourdain³

¹Department of Meteorology, Stockholm University, Stockholm, Sweden

²Bolin Centre for Climate Research, Stockholm, Sweden

³Univ. Grenoble Alpes/CNRS/IRD/G-INP/INRAE, IGE, Grenoble, France

Correspondence: Jonathan Wiskandt (jonathan.wiskandt@misu.su.se)

Abstract.

Basal melt of marine terminating glaciers is a key uncertainty in predicting the future climate and the evolution of the Antarctic and Greenland ice sheets. Regional ocean circulation models use parameterizations that depend on the available heat to parameterize basal melt. The heat budget at the ice–ocean interface includes turbulent heat flux from the ocean below, latent heat for phase transition, and heat conduction into the ice. Here we review the estimation of heat conduction into the ice, which has been treated in various ways in modelling studies so far. We show that the formulation of Holland and Jenkins (1999) best captures the variety of temperature profiles measured in boreholes. Accounting for heat conduction into the ice reduces melt rates by up to 28%.

1 Introduction

In ocean general circulation models (OGCM), marine terminating glaciers are usually assumed static and the local melt rate is parameterized using a set of three equations consisting of a linearization of the local freezing point temperature of water, as well as heat and salt budgets at the ice–ocean interface (Holland and Jenkins, 1999). The turbulent transport of heat from the water to the ice–ocean interface is partly balanced by the heat conduction into the ice. Any excess of heat from the combination of these two processes is used as latent heat for the solid to liquid melt change. Hence, a good representation of ice shelf basal melting in ocean models requires accurate simulations of both the turbulent heat transport in the water below the ice and the heat conduction into the ice shelf.

Heat conduction into the ice has often been neglected in ocean simulations resolving ice shelf cavities, with the idea that the resulting bias does not affect melt rates by more than 10% (Dinniman et al., 2016; Comeau et al., 2022). Other models have adopted a crude representation of this flux, by assuming a linear temperature profile between the freezing temperature at ice shelf base and a typical annual mean air temperature at the ice shelf surface (e.g., Losch, 2008; Mathiot et al., 2017). More than 60 years ago, Wexler (1960) proposed a more elaborated formulation of this conductive heat flux by accounting for heat advection by the vertical ice motion, based on the observation of a few vertical temperature profiles. The formulation was completed by Holland and Jenkins (1999) who proposed a linear approximation of Wexler’s solution so that it can be incorporated in the solution of the three-equation system used to estimate basal melt rates in ocean models.



25 In this brief communication, we review these approaches, discuss their accuracy for realistic applications, and estimate the influence of heat conduction on ice shelf basal melt rates around Antarctica. Finally, we propose future directions to improve the calculation of these fluxes in ocean or Earth system models.

2 Assessment of the various approaches

The heat budget at the ice–ocean interface that is used to derive melt rates in ocean models can be expressed as:

$$30 \quad mL = \rho_w c_w u_* \Gamma_T (T_w - T_{z_d}) + \rho_i c_i \kappa_i \left(\frac{\partial T_i}{\partial z} \right)_{z_d} \quad (1)$$

where m is the melt rate expressed in $\text{kg m}^{-2} \text{s}^{-1}$ (negative in case of refreezing), ρ_w and ρ_i the densities of seawater and ice, L the melting/freezing latent heat of water, c_w and c_i the heat capacity of seawater and ice, u_* the friction velocity calculated by the ocean model, κ_i the heat conductivity of ice, T_i the ice temperature, T_w the ocean temperature at some distance from the ice–ocean interface, T_{z_d} the local freezing point temperature, and z_d the ice draft vertical position (z negative below sea level and increasing upward).

The three common approximations made in ocean models to deal with heat conduction in the ice are:

$$\left\{ \begin{array}{l} \rho_i \kappa_i \left(\frac{\partial T_i}{\partial z} \right)_{z_d} = 0 \quad (A) \\ \rho_i \kappa_i \left(\frac{\partial T_i}{\partial z} \right)_{z_d} = \rho_i \kappa_i \frac{T_s - T_{z_d}}{z_s - z_d} \quad (B) \\ \rho_i \kappa_i \left(\frac{\partial T_i}{\partial z} \right)_{z_d} = (T_s - T_{z_d}) \max\{m, 0\} \quad (C) \end{array} \right. \quad (2)$$

where T_s is the ice surface temperature at height z_s , ρ_0 the density of pure water.

Approximation (A) in eq. (2) would be a good approximation if there were ice shelves close to the ocean freezing point over their entire thickness, but such ice shelves are likely unstable (Morris and Vaughan, 2003). It can still be a reasonable approximation for locations where ice shelves have a layer of marine ice at their base (Fig. 1a), although the permeable nature of this type of ice makes proper calculations complicated (Wang et al., 2022).

Approximation (B) in eq. (2) assumes no heat advected by the ice and a temperature profile that has reached a steady state between the freezing temperature at the base and a constant surface temperature. This seems to be a good approximation for the Ross Ice Shelf (RIS, Fig. 1b). The ice typically takes 1,000 years to go from the grounding line to the borehole of the shown temperature profile (MacAyeal and Thomas, 1979; Mouginit et al., 2019), which corresponds to the typical time taken by heat to be conducted from the surface or the base to the middle of a 400 m thick ice shelf (estimated as $(H/2)^2/\kappa_i$ where H is the ice thickness). The ice may take less than a century to cross some of the smaller ice shelves of similar thickness (Mouginit et al., 2019), which makes it unlikely that a thermal steady state is reached for these other ice shelves. Furthermore, Ross is characterized by very low basal melt rates (MacAyeal and Thomas, 1979; Rignot et al., 2013) and relatively low accumulation

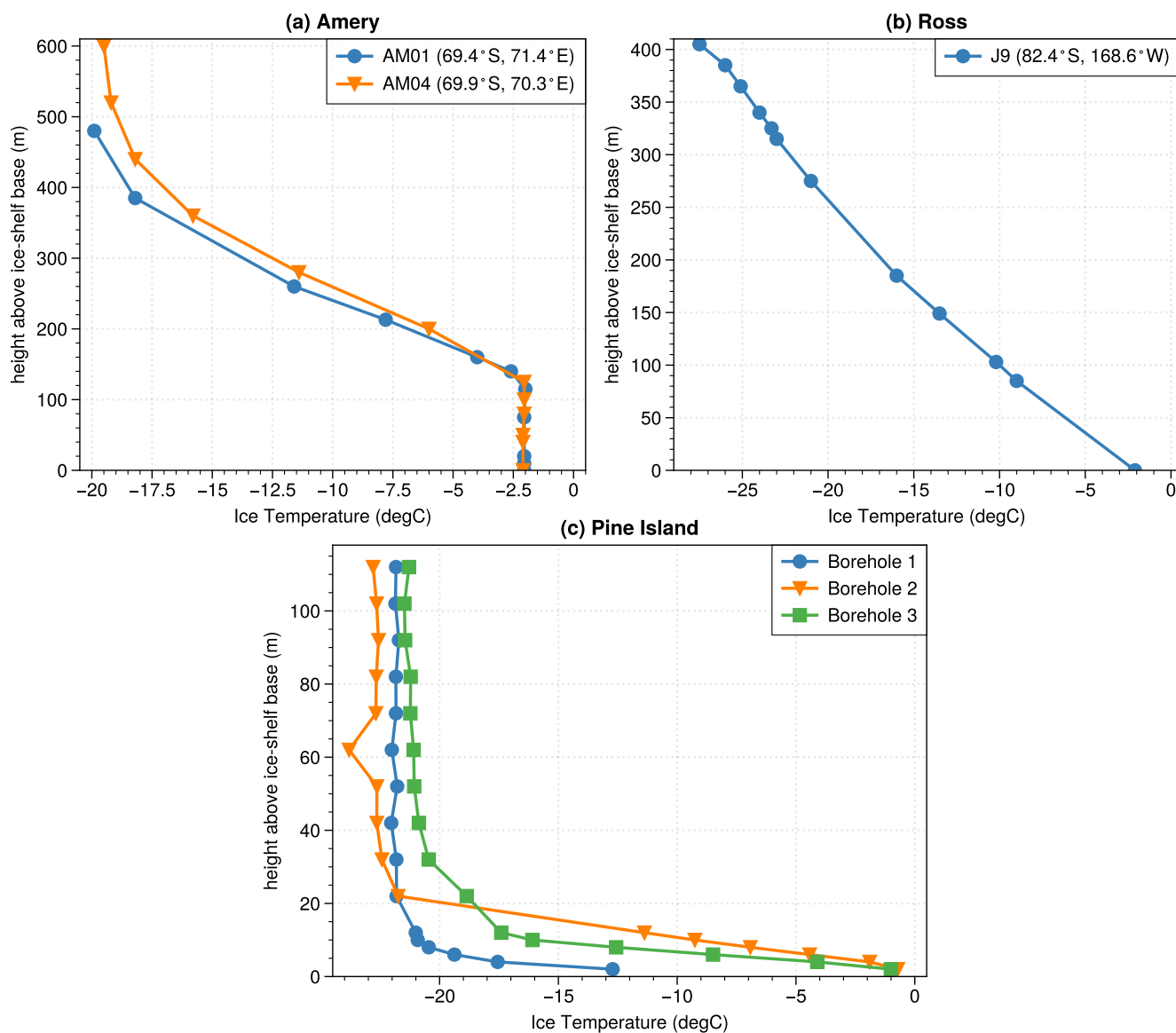


Figure 1. Ice temperature profiles measured by thermistor strings in boreholes at (a) two sites on Amery Ice Shelf (69.4°S, 71.4°E and 69.9°S, 70.3°E; respectively AM01 and AM04 in Wang et al., 2022) (b) one site in the middle of the Ross Ice Shelf (168.6°W, 82.4°S; J9 in MacAyeal and Thomas, 1979), and (c) three sites on Pine Island Ice Shelf (105.1°W, 75.1°S; Truffer and Stanton, 2015). A layer of marine ice is present underneath the ice shelf at sites AM01 and AM04 (more than 100 m thick) and at site J9 (6 m thick).

rate at the surface (Agosta et al., 2019), which is expected to result in relatively low ice vertical velocities. Therefore, the thermal regime is very different for small ice shelves with high melt rates at their base, such as the Pine Island Ice Shelf, characterized by a strong temperature gradient at the base (Fig. 1c).



Approximation (C) in eq. (2) is made to account for vertical heat advection and was obtained by Holland and Jenkins (1999).
55 They considered a vertical ice velocity directly proportional to the basal melt rate, i.e., they assumed that the melted ice was
instantaneously compensated by surface accumulation or ice flow convergence, which is correct for a constant ice shelf shape.
The formulation of eq. (2C) is a linearization of a more complex expression that tends to zero for refreezing rates greater than
 ~ 0.1 meters of ice per year (Holland and Jenkins, 1999). This formulation represents strong ice temperature gradients at the
ice shelf base, and strong associated melt rates. Here, a steady state is still assumed, but the characteristic time to reach the
60 steady state is imposed by the basal melt rate and not by heat conduction. The typical aspect ratio and horizontal ice velocities
make this approximation reasonable for many ice shelves of Antarctica and Greenland (Rignot et al., 2013; Mouginit et al.,
2019).

When considering the variety of ice temperature profiles found in Antarctic (Fig. 1a-c), it appears that approximation (A)
only works in the presence of refreezing (Fig. 1a) while approximation (B) only works for large ice shelves with very weak
65 basal melt rates (Fig. 1b). Approximation (C) appears as the only one able to represent the variety of temperature profiles.
In case of refreezing ($m < 0$ in eq. (2C)), no heat is conducted into the ice (Fig. 2a), which is consistent with the vertical
temperature profiles observed in the marine ice layer beneath the Amery Ice Shelf (Fig. 1a). In case of actual melting ($m > 0$
in eq. (2C)), the conductive heat flux is proportional to melt rates, consistently with the strong temperature gradients observed
at the base of Pine Island ice shelf. The range of very weak melt rates ($-0.05 < m < 0.05$ m yr⁻¹) is the only one where the
70 linear temperature profile is a better approximation than the linearization of Holland and Jenkins (Fig. 2a).

If we assume positive melt rates and use eq. (2C) in eq. (1), we can estimate the relative error in melt rates made when
neglecting heat conduction, i.e., when using approximation (A) compared to approximation (C):

$$\frac{\Delta m}{m} = \frac{c_i (T_s - T_{zd})}{L} \quad (3)$$

Considering the parameter values used in Holland and Jenkins (1999), melt rates calculated without considering heat con-
75 duction in the ice are overestimated by 11% for a surface temperature of -20°C and a freezing point temperature of -2°C at the
ice base. The overestimation is very similar when using the linear temperature profile rather than nothing, except in the absence
of basal melting.

We now estimate the effect of conduction for all Antarctic ice shelves in climatological conditions. Applying eq. (3) to the
observational melt rates of Rignot et al. (2013) gives an idea of where errors due to underestimation of the heat flux have the
80 largest effects (Fig. 3). We use the 40-year (1980-2019) average snow surface temperatures from a regional climate simulation
(Kittel et al., 2021) as T_s and calculate the pressure dependent freezing point temperature T_{zd} using BedMachine (Morlighem
et al., 2020) data and a typical salinity of 34.6 g kg⁻¹ everywhere. Most areas show a difference of around 12% with higher
values seen at Amery Ice Shelf (AmIS) and the eastern Ross Ice Shelf (RIS, both above 27%). In the most part of RIS this
translates to only small differences in absolute numbers (below 0.1 m yr⁻¹, Fig. 3b), since melt rates here are very low (Rignot
85 et al., 2013). In crucial areas, such as close to the grounding lines of Filchner-Ronne Ice Shelf (FRIS), most of AmIS and the
smaller ice shelves draining towards the Amundsen Sea, the error is multiple meters per year, surpassing even 10 m yr⁻¹ at
Pine Island Glacier and AmIS. At the calving fronts of FRIS and RIS errors are around 1 m yr⁻¹.

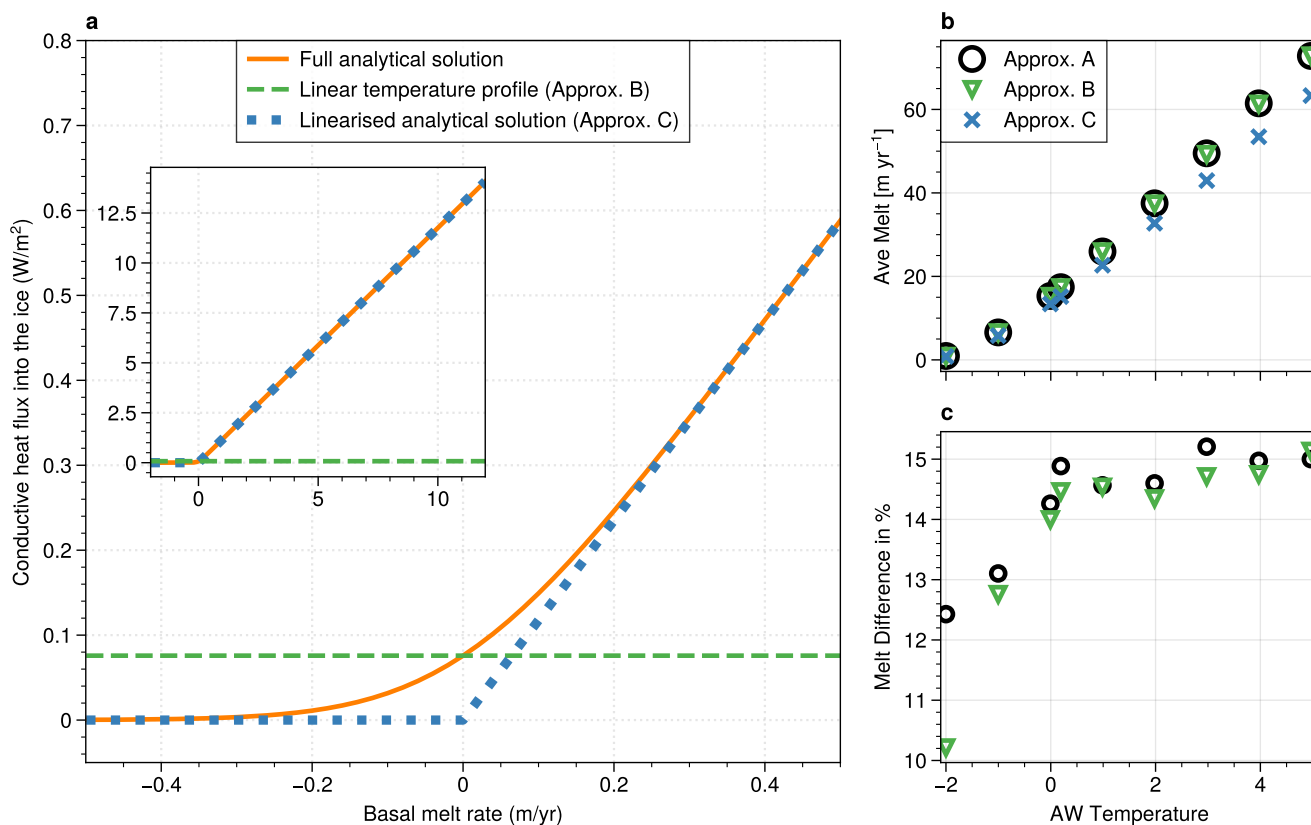


Figure 2. a) Conductive heat flux at the ice shelf base as a function of the basal melt rate expressed in meters of ice per year. The inset shows the same lines but with a broader range of melt rates. The blue line is the full analytical solution provided by Holland and Jenkins (1999), the dashed orange line is the linear simplification that they suggest (approximation C in eq. 2), and the green line is derived from the assumption of a linear temperature profile across the ice shelf thickness (approximation B in eq. 2). b) Simulated average melt rate from identical MITgcm ocean simulations using the three different approximations of eq. 2 as a function of bottom layer ocean Temperature. c) Melt rate difference with respect to Approximation C.

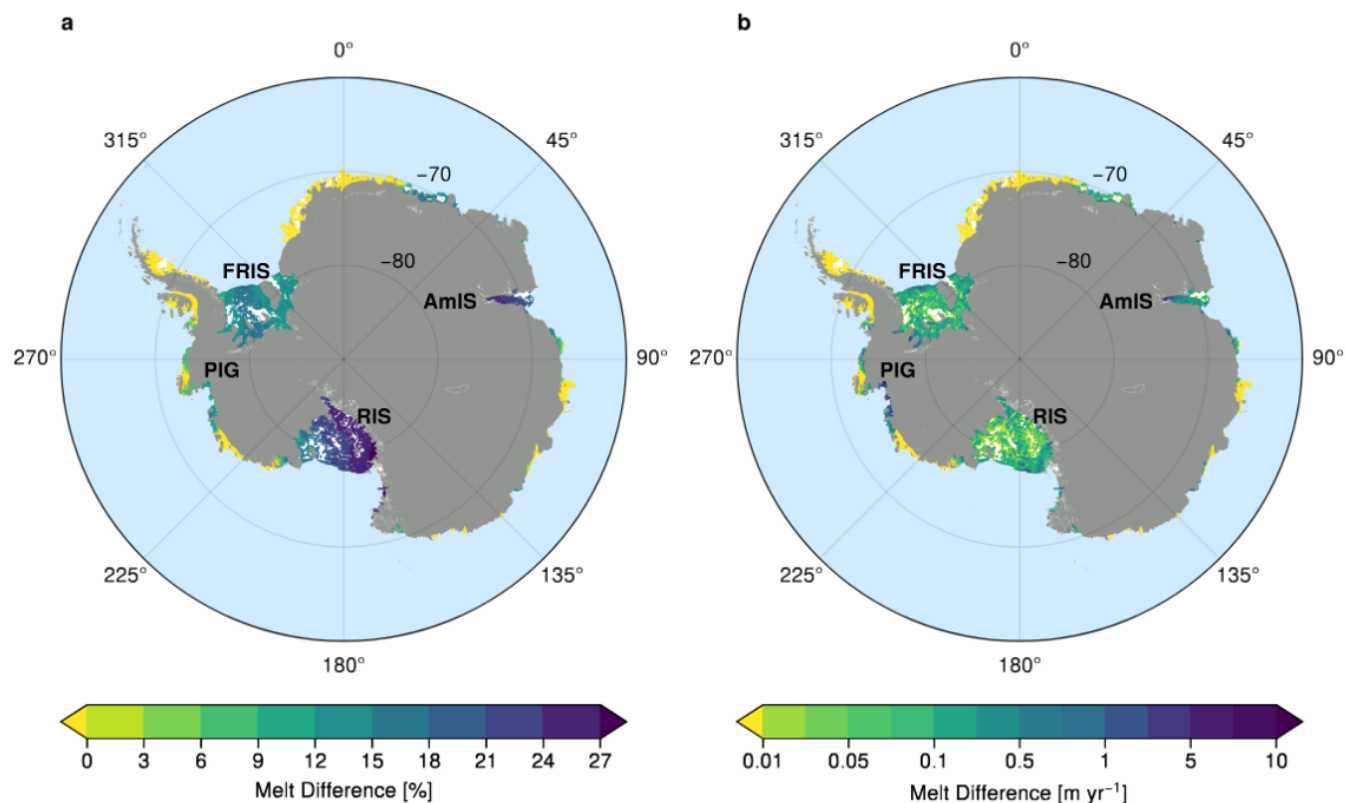


Figure 3. Map of Antarctica showing relative melt rate differences (Eq. 3) between Approximation 2A and 2C and respective absolute values when applied to melt rate data for floating ice shelves (b). White areas indicate regions of refreezing.

3 Application to ocean simulations of a small cavity

For a practical implementation of approximation (C) in an ocean model, the criterion on m to bound the heat conduction to zero is not very convenient, as this would require some iterations of the three-equation system because m is a solution that is not known a priori. A more practical solution is to check the sign of the thermal forcing ($T_w - T_{zd}$ in eq. 1) to decide whether or not heat conduction is set to zero. This is not perfectly equivalent, as a slightly positive thermal forcing may allow for refreezing due to heat loss through heat conduction in the ice, but in the large majority of cases, this will be equivalent. In the next section, we test this implementation in the MITgcm ocean model (Adcroft et al., 2004) and evaluate whether the relative importance of heat conduction, as derived from the theory, is still valid in the presence of a realistic ocean circulation and possible ice-ocean feedbacks.

To show the differences between the three approaches in the melt parametrization in a regional circulation model, we set up a suite of idealized, 2D, non-rotational simulations (Wiskandt et al., 2023) in MITgcm with varying ocean temperatures comparing the three different approaches introduced in eq. 2. The geometry is representative of a long and narrow fjord,



100 typically found around Greenland. The Domain is 30 km long and 1 km deep with an ice shelf covering the first 20 km of the domain with a grounding line depth of 950 m and a 50 m deep vertical front. Note that none of the present simulations exhibits refreezing. For all details of the simulation refer to Wiskandt et al. (2023).

In line with Fig. 2a, simulated melt rates are very similar when using approximation (A) or (B) in eq. 2 (Fig. 2b-c). Although absolute melt rates are barely discernible by eye here, relative differences show a change below 1% for the entire simulated
105 temperature range, except for the coldest (Fig. 2c). The error made by both approximation (A) and (B) lays between 10-15% where most experiments, i.e. those with temperature ≤ 0 show an error of 14-15%.

4 Conclusions

Former ocean circulation studies at both Greenlandic and Antarctic marine terminating glaciers implement approximation (A) (e.g. Gwyther et al., 2020; Comeau et al., 2022) or (B) (e.g. De Rydt and Naughten, 2024; Wiskandt et al., 2023; Holland et al.,
110 2008; Losch, 2008) in eq. 2 for heat conduction into the ice. As shown above, both these approaches overestimate melt rates by more than 12% depending on the ice surface temperature, the ice shelf geometry (see eq. 3) and the temperature profile in the ice. Only approximation (C) is able to accurately estimate the heat flux for a variety of different ice temperature profile.

Instead of using the more accurate approximation (C) for the heat flux to model the melt rate, modellers tune melt rates to observations by adjusting the drag coefficient (i.e. the friction velocity in eq. 1). This changes the melt uniformly everywhere
115 but does not account for spatial variability of the error. Especially in the grounding line region, where changes in ice shelf geometry can trigger rapid ice loss, accurate melt rates are crucial to estimate the stability of the ice shelf (De Rydt and Naughten, 2024). In ocean circulation models, a melt-dependent local temperature gradient is straightforward to implement and, in fact, available in MITgcm in the SHELFICE package (Losch, 2008). The Finite-volume Sea ice–Ocean Model (FESOM2) (Danilov et al., 2017) already uses an approach similar to approximation (C), with a slightly different implementation of refreezing than
120 what we propose above.

The parameterizations using a linear dependency of the heat flux on the melt rate has been identified as the best available, but it is nonetheless based on several approximations Holland and Jenkins (1999). To accurately model the ice-ocean interactions, a coupled ice-sheet–ocean model should be used, with a representation of both heat conduction and heat advection in ice. A large part of the current ice-sheet models however, do not explicitly simulate the ice-sheet temperatures and sometimes
125 use approximations of the Stokes equation that prevent a good representation of vertical heat advection in ice (e.g. Seroussi et al., 2020). Hence, we suggest that coupled models currently under development should consider calculating the ice sheet temperature gradients or heat fluxes and transfer them into the ocean model to accurately calculate the melt rate using the three-equation system. For non–coupled models the authors strongly suggest to implement approach (C) of eq. 2 when parameterizing marine basal melt, as it more accurately represents the heat conduction into the ice and comes at no additional computational
130 cost.



Code and data availability. The configuration files necessary to reproduce the simulations used in the present study employed the MITgcm (downloaded in 2020 from <https://github.com/MITgcm/MITgcm/releases/tag/checkpoint67s>, last access: 4 July 2023), and are/will be available through the Bolin Research Centre Data Centre (<https://doi.org/10.17043/wiskandt-2024-sof-sill-1>). Also available are/will be time averaged fields and key diagnostics from the simulations and all data and code needed to reproduce the shown figures.

135 *Author contributions.* JW and NCJ initiated this work and reviewed the theory together. JW ran the MITgcm simulations and analysed the results. All authors discussed the results and contributed to the manuscript.

Competing interests. Nicolas Jourdain is an editor of The Cryosphere.

Acknowledgements. NCJ's contribution was supported by the European Union's Horizon 2020 research and innovation programme (EU-H2020) under grant agreement No 101003536 (ESM2025), and by the Agence Nationale de la Recherche - France 2030 as part of the
140 PEPR TRACCS programme under grant number ANR-22-EXTR-0010. JW's work was performed within a pair PhD project funded by the Faculty of Science, Stockholm University, and granted to the Department of Mathematics, division of Computational Mathematics, and the Department of Meteorology (SUFV-1.2.1-0124-17). The MITgcm simulations were enabled by resources provided by the National Academic Infrastructure for Supercomputing in Sweden (NAISS) at the National Supercomputer Centre (NSC), partially funded by the Swedish Research Council through grant agreements no. 2022-06725.



145 References

- Adcroft, A. J., Hill, C., Campin, J. M., Marshall, J., and Heimbach, P.: Overview of the formulation and numerics of the MIT GCM, in: Proceedings of the ECMWF seminar series on Numerical Methods, Recent developments in numerical methods for atmosphere and ocean modelling, pp. 139–149, ECMWF, URL: <https://www.ecmwf.int/en/elibrary/7642-overview-formulation-and-numerics-mit-gcm>, 2004.
- Agosta, C., Amory, C., Kittel, C., Orsi, A., Favier, V., Gallée, H., van den Broeke, M. R., Lenaerts, J., van Wessem, J. M., van de Berg, W. J., et al.: Estimation of the Antarctic surface mass balance using the regional climate model MAR (1979–2015) and identification of dominant processes, *The Cryosphere*, 13, 281–296, 2019.
- 150 Comeau, D., Asay-Davis, X. S., Begeman, C. B., Hoffman, M. J., Lin, W., Petersen, M. R., Price, S. F., Roberts, A. F., Van Roekel, L. P., Veneziani, M., et al.: The DOE E3SM v1.2 cryosphere configuration: Description and simulated Antarctic ice-shelf basal melting, *Journal of Advances in Modeling Earth Systems*, 14, e2021MS002468, 2022.
- 155 Danilov, S., Sidorenko, D., Wang, Q., and Jung, T.: The Finite-volume Sea ice–Ocean Model (FESOM2), *Geoscientific Model Development*, 10, 765–789, <https://doi.org/10.5194/gmd-10-765-2017>, 2017.
- De Rydt, J. and Naughten, K.: Geometric amplification and suppression of ice-shelf basal melt in West Antarctica, *The Cryosphere*, 18, 1863–1888, <https://doi.org/10.5194/tc-18-1863-2024>, 2024.
- Dinniman, M. S., Asay-Davis, X. S., Galton-Fenzi, B. K., Holland, P. R., Jenkins, A., and Timmermann, R.: Modeling ice shelf/ocean interaction in Antarctica: A review, *Oceanography*, 29, 144–153, 2016.
- 160 Gwyther, D. E., Kusahara, K., Asay-Davis, X. S., Dinniman, M. S., and Galton-Fenzi, B. K.: Vertical processes and resolution impact ice shelf basal melting: A multi-model study, *Ocean Modelling*, 147, 101569, <https://doi.org/10.1016/j.ocemod.2020.101569>, publisher: Elsevier Ltd., 2020.
- Holland, D. M. and Jenkins, A.: Modeling thermodynamic ice-ocean interactions at the base of an ice shelf, *Journal of Physical Oceanography*, 29, 1787–1800, [https://doi.org/10.1175/1520-0485\(1999\)029<1787:mtioia>2.0.co;2](https://doi.org/10.1175/1520-0485(1999)029<1787:mtioia>2.0.co;2), 1999.
- 165 Holland, P. R., Jenkins, A., and Holland, D. M.: The response of Ice shelf basal melting to variations in ocean temperature, *Journal of Climate*, 21, 2558–2572, <https://doi.org/10.1175/2007JCLI1909.1>, 2008.
- Kittel, C., Amory, C., Agosta, C., Jourdain, N. C., Hofer, S., Delhasse, A., Doutreloup, S., Huot, P.-V., Lang, C., Fichet, T., and Fettweis, X.: Diverging future surface mass balance between the Antarctic ice shelves and grounded ice sheet, *The Cryosphere*, 15, 1215–1236, <https://doi.org/10.5194/tc-15-1215-2021>, 2021.
- 170 Losch, M.: Modeling ice shelf cavities in a z coordinate ocean general circulation model, *Journal of Geophysical Research: Oceans*, 113, 1–15, <https://doi.org/10.1029/2007JC004368>, 2008.
- MacAyeal, D. R. and Thomas, R. H.: Ross Ice Shelf temperatures support a history of ice-shelf thickening, *Nature*, 282, 703–705, 1979.
- Mathiot, P., Jenkins, A., Harris, C., and Madec, G.: Explicit representation and parametrised impacts of under ice shelf seas in the z* coordinate ocean model NEMO 3.6, *Geoscientific Model Development*, 10, 2849–2874, 2017.
- 175 Morlighem, M., Rignot, E., Binder, T., Blankenship, D., Drews, R., Eagles, G., Eisen, O., Ferraccioli, F., Forsberg, R., Fretwell, P., Goel, V., Greenbaum, J. S., Gudmundsson, H., Guo, J., Helm, V., Hofstede, C., Howat, I., Humbert, A., Jokat, W., Karlsson, N. B., Lee, W. S., Matsuoka, K., Millan, R., Mouginit, J., Paden, J., Pattyn, F., Roberts, J., Rosier, S., Ruppel, A., Seroussi, H., Smith, E. C., Steinhage, D., Sun, B., Broeke, M. R. V. D., Ommen, T. D. V., Wessem, M. V., and Young, D. A.: Deep glacial troughs and stabilizing ridges unveiled beneath the margins of the Antarctic ice sheet, *Nature Geoscience*, 13, 132–137, <https://doi.org/10.1038/s41561-019-0510-8>, 2020.
- 180



- Morris, E. M. and Vaughan, D. G.: Spatial and temporal variation of surface temperature on the Antarctic Peninsula and the limit of viability of ice shelves, *Antarctic Research Series*, 79, 2003.
- Mouginot, J., Rignot, E., and Scheuchl, B.: Continent-wide, interferometric SAR phase, mapping of Antarctic ice velocity, *Geophysical Research Letters*, 46, 9710–9718, 2019.
- 185 Rignot, E., Jacobs, S., Mouginot, J., and Scheuchl, B.: Ice-shelf melting around Antarctica, *Science*, 341, 266–270, 2013.
- Seroussi, H., Nowicki, S., Payne, A. J., Goelzer, H., Lipscomb, W. H., Abe Ouchi, A., Agosta, C., Albrecht, T., Asay-Davis, X., Barthel, A., et al.: ISMIP6 Antarctica: a multi-model ensemble of the Antarctic ice sheet evolution over the 21 st century, *The Cryosphere Discussions*, 2020, 1–54, 2020.
- Truffer, M. and Stanton, T.: Borehole Temperatures at Pine Island Glacier, Antarctica, Tech. rep., U.S. Antarctic Program (USAP) Data Center, <https://doi.org/10.7265/N5T151MV>, 2015.
- 190 Wang, Y., Zhao, C., Gladstone, R., Galton-Fenzi, B., and Warner, R.: Thermal structure of the Amery Ice Shelf from borehole observations and simulations, *The Cryosphere*, 16, 1221–1245, 2022.
- Wexler, H.: Heating and melting of floating ice shelves, *Journal of Glaciology*, 3, 626–645, 1960.
- Wiskandt, J., Koszalka, I. M., and Nilsson, J.: Basal melt rates and ocean circulation under the Ryder Glacier ice tongue and their response to climate warming: a high-resolution modelling study, *The Cryosphere*, 17, 2755–2777, <https://doi.org/10.5194/tc-17-2755-2023>, 2023.
- 195